Ceramics International 45 (2019) 10930–10935

Contents lists available at ScienceDirect

Ceramics International

journal homepage: www.elsevier.com/locate/ceramint

Rapid preparation of dense $Gd_2Zr_2O_7$ nano-grain ceramics by microwave sintering in air

Mao Zhou[a,b], Zhangyi Huang[a,b], Nannan Ma[a,b], Jianqi Qi[a,b,*], Haibin Zhang[d], Xiaofeng Guo[e,f,**], Di Wu[f,g], Yutong Zhang[a,b], Tiecheng Lu[a,b,c,***]

[a] College of Physical Science and Technology, Sichuan University, Chengdu, 610064, China
[b] Key Laboratory of Radiation Physics and Technology of Ministry of Education, Sichuan University, Chengdu, 610064, China
[c] Key Laboratory of High Energy Density Physics of Ministry of Education, Sichuan University, Chengdu, 610064, China
[d] Institute of Nuclear Physics and Chemistry, China Academy of Engineering Physics, Mianyang, 621900, China
[e] Department of Chemistry, Washington State University, Pullman, WA, 99164, United States
[f] Alexandra Navrotsky Institute for Experimental Thermodynamics, Washington State University, Pullman, WA, 99164, United States
[g] The Gene and Linda Voiland School of Chemical Engineering and Bioengineering, Washington State University, Pullman, WA, 99164, United States

ARTICLE INFO

Keywords:
$Gd_2Zr_2O_7$ nanoceramics
Microwave sintering
Pressureless method
Densification behavior

ABSTRACT

$Gd_2Zr_2O_7$ nano-grain ceramics with high densities (> 90%) and small average grain sizes (66–96 nm) were successfully fabricated for the first time by the fast microwave pressureless sintering method (processing time: 10–90 min). The sintering behavior and microstructural evolution of fluorite structure $Gd_2Zr_2O_7$ nano-grain ceramics were investigated from 1100 °C to 1300 °C. Comparative analyses were conducted to unveil the influence of temperature and holding time on densification. The results suggest the optimized conditions for sintering dense nano-grain ceramics (66–96 nm) can be achieved at relatively low temperatures (< 1250 °C) and long sintering time (60–90 min), or at high temperatures (> 1250 °C) and short sintering time (10–60 min). As a demonstration, dense $Gd_2Zr_2O_7$ ceramics with average grain size of 66 nm were prepared for the first time by rapid microwave pressureless sintering.

1. Introduction

Crystalline ceramic materials have been reported as promising solid-form candidates for immobilizing radionuclides due to the high resistance to radiation and high chemical stability compared to glass solidified bodies [1–5]. Particularly, nanocrystalline ceramics (grain sizes < 100 nm) were found to have higher radiation tolerance than microcrystalline counterparts, due to the abundance of grain boundaries and interfaces that can absorb defects and eliminate vacancies [6–8]. For example, small-grained $MgGa_2O_4$ ceramics with average grain size below 12 nm can still remain crystalline under Kr^+ ion irradiation with a fluence of 4×10^{20} Kr/m^2, while large-grained samples (> 100 nm) are amorphized by a fluence of 5×10^{19} Kr/m^2 [9]. Nanocrystalline yttria stabilized zirconia (YSZ) and $Gd_2(Ti_{0.65}Zr_{0.35})_2O_7$ also display enhanced radiation resistance compared to their coarse-grained counterparts [10,11]. Particularly, $Gd_2Zr_2O_7$ can crystallize in both pyrochlore and defect-fluorite structures, and its ceramic form has been proposed as an ideal waste matrix for immobilizing radionuclides. The superior radiation resistance of the gadolinium-zirconate system is mostly attributed to the high neutron cross section of Gd and the high structural resistance to the radiation damage [12,13]. Moreover, the high density of ceramics also favors the waste disposal application due to the improved mechanical strength and the decreased penetration from solid interfaces [14,15], which also motivates us to study the fabrication of nanocrystalline $Gd_2Zr_2O_7$ ceramics in this work.

Dense nano-grain ceramics (~90%, < 100 nm) can be prepared by hot press sintering or field assisted sintering technique [15–18]. However, pressure-assisted sintering is economically too demanding in terms of both cost and supporting facilities. Therefore, pressureless sintering has attracted research interests in recent years due to its simple experimental setup and low cost. In our previous study [19], nano-grain $Gd_2Zr_2O_7$ ceramics with high density were successfully synthesized by using an unprecedentedly simple and effective pressureless two-step sintering method. However, this method requires

* Corresponding author. College of Physical Science and Technology, Sichuan University, Chengdu, 610064, China.
** Corresponding author. Department of Chemistry, Washington State University, Pullman, WA, 99164, United States.
*** Corresponding author. College of Physical Science and Technology, Sichuan University, Chengdu, 610064, China.
E-mail address: qijianqi@scu.edu.cn (J. Qi).

https://doi.org/10.1016/j.ceramint.2019.02.173
Received 4 September 2018; Received in revised form 24 February 2019; Accepted 24 February 2019
Available online 25 February 2019

excessive sintering time (~20 h). Thus, a pressureless sintering approach optimizing the sintering time is needed for industrial-scale fabrication of waste-encapsulated ceramics.

To achieve high density nanocrystalline ceramics in short sintering time, microwave sintering has been preferably used compared to conventional sintering for performing rapid sintering of high density ceramics (Al_2O_3, ZrO_2, Al_2O_3, ZnO, etc.) [19–25]. During microwave sintering, the sample can directly absorb the electromagnetic energy and convert it to heat, which is controlled by the dielectric interaction between the sample and the electric field. Particularly, by changing microstructures, including grain boundaries, porosities, defects, and impurities, one can shift the dielectric loss of the material [26,27] and the converting ability [28], and thus control the microwave sintering process. The advantages of microwave sintering include: *i*) expediting the diffusion process, *ii*) reducing the sintering activation energy, and *iii*) accelerating the mass transport. These advantages allow us to perform sintering at lower temperatures and shorter sintering time to fabricate densified samples with fine grains and uniform microstructures [28–32]. In addition, using fine powders with improved dielectric properties can also reduce the sintering temperature that helps fabricate nano-grained ceramics [33]. However, there are no studies on the microwave sintering of dense (> 90%) nano grain-sized (< 100 nm) $Gd_2Zr_2O_7$ ceramics under air atmosphere. Recently, Lu et al. successfully prepared high density $Gd_2Zr_2O_7$ ceramics by a short-time microwave sintering process [34]. However, the fabricated sample has large grains (> 2.4 μm). Thus, as a continuing study of our previous work on pressureless sintering method [19], we aimed at further shortening the sintering time so that dense $Gd_2Zr_2O_7$ ceramics can be prepared with smaller grain sizes. Specifically, we emphasized the effects of sintering temperature and time on grain size and relative density of $Gd_2Zr_2O_7$ ceramics during the microwave sintering processing. As a result of this work, nano grain-sized samples were obtained after a short sintering time (< 90 min). The pressureless microwave sintering method would open up a new challenge to the ceramic technologists to understand the dielectric interaction mechanism between the ceramics and applied electric field to fabricate the tailor-made high density refractory nanoceramics.

2. Experimental procedure

2.1. Synthesis procedure

$Gd_2Zr_2O_7$ powders with ultra-fine nanocrystals were synthesized by a modified solvothermal method, which was described in our previous work [19,35]. The nano-sized powders obtained from the calcination treatment at 500 °C for 2 h were uniaxially pressed into green pellets with a diameter of 10 mm and a thickness of 2 mm–3 mm. To synthesize green bodies with higher homogeneity, cold isostatic pressing was applied at 200 MPa. Then the green pellets with a relative density of 54% were sintered at 1100°C-1300 °C for different sintering time. A fixed heating rate of 15 °C/min was provided by the electromagnetic field.

2.2. Sintering procedure

The microwave sintering system (RWS3H, China) with a single mode cavity (450 cm × 450 cm × 530 cm) was operating at 2.45 GHz. An infrared pyrometer (MI3-2M-SF1) installed above the cavity can measure temperature (250°C-1400 °C) during the sintering. The samples were placed into a cylindrical crucible made of alumina fibers [26]. Because of the low dielectric loss factor of $Gd_2Zr_2O_7$ nano-grain ceramics at low sintering temperature, SiC pellets as auxiliary heaters were placed around the sample crucible for providing uniform heating upon absorption of microwaves.

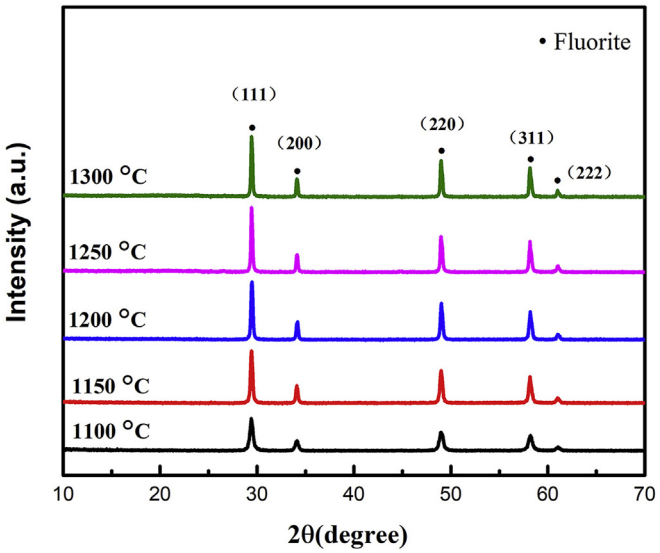

Fig. 1. XRD patterns for the $Gd_2Zr_2O_7$ nanoceramics synthesized at different temperatures for 30 min.

2.3. Analytical procedure

The phases of sintered ceramics were characterized by a powder X-ray diffractometer (PXRD, Model DX-2700, Dandong Fangyuan Instrument Co, Ltd, Liaoning, China) with Cu-Kα radiation in a wide range of 2θ (10°–70°) at a scanning rate of 1.8°/min. The microstructures were investigated by a scanning electron microscopy (SEM, Model S-4800, Hitachi, Japan). The average grain size was determined by integrating and computing the visible grains from the SEM images using Nanomeasure software. The relative density was determined by the Archimedes method with ethyl alcohol as the immersion medium.

3. Results and discussion

The XRD patterns of $Gd_2Zr_2O_7$ ceramics sintered at different temperatures (1100°C-1300 °C) for 30 min are shown in Fig. 1. All peaks are in good matches with reference indices of the defect-fluorite phase (JCPDS #80–0471), and there are no observable phase transformations over the whole temperature range. The low temperature sintered phase is of nano grain-sized, which was quantified by fitting the diffraction peaks using the Scherrer equation. With increasing the sintering temperature, sharpening of peaks was observed as a consequence of crystalline growth. The nanosized crystallinity favors the formation of the defect-fluorite phase over the pyrochlore phase [36]. This is because as size decreases, more energetic contributions come from the surfaces and the interfaces that shift the total energy of the pyrochlore phase higher. Thus, it is reasonable that we did not observe a phase transition from defect-fluorite to pyrochlore structure, which occurs in bulk $Gd_2Zr_2O_7$ at high sintering temperatures (> 1300 °C) [37].

The microstructures of ceramics sintered at different temperatures are shown in Fig. 2. In our previous work [19], a conventional sintering method was used at 1250 °C for 10 h that yielded $Gd_2Zr_2O_7$ nanoceramics with an average grain size of 90 nm and 80% relative density. As a great improvement in this work, we performed microwave sintering under 1250 °C for a much shorter sintering time (30 min), but produced ceramics with smaller grains (88 nm) and fewer porosities (92%) (Fig. 2(d)). The only drawback is the low relative density of the obtained sample pellets (~54%), lower than that obtained from conventional sintering [19], which however, can be improved by increasing the sintering temperature. As temperature increases to 1300 °C (Fig. 2(e)), the relative density can reach 93%, and the sample has a homogenous microstructure with low porosity and a narrow

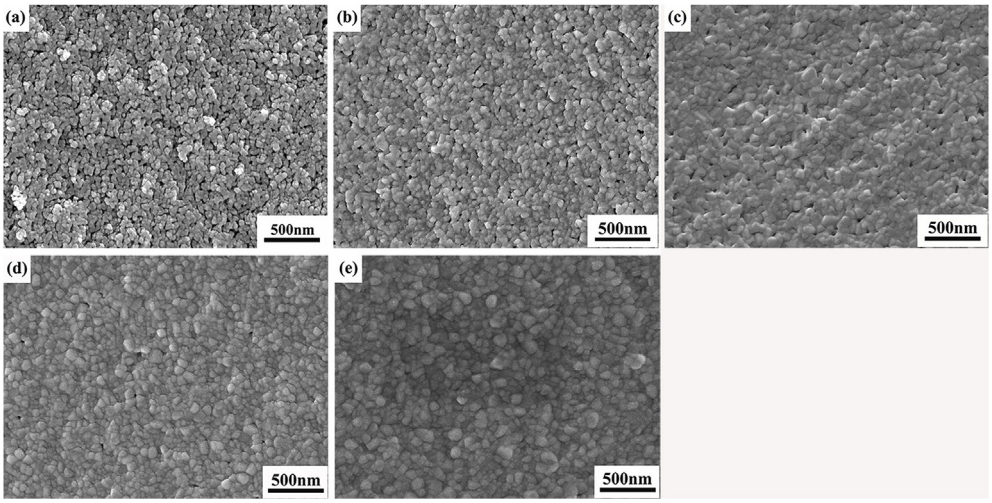

Fig. 2. Scanning electron microscopy (SEM) images of $Gd_2Zr_2O_7$ ceramics sintered for 30 min at (a) 1100 °C, (b) 1150 °C, (c) 1200 °C, (d) 1250 °C and (e) 1300 °C.

distribution of grain sizes (~ 96 nm). On the contrary, samples sintered at 1100 °C, 1150 °C, and 1200 °C all showed relatively low densification with small grains. This is because at low temperature the poor dielectric performance of $Gd_2Zr_2O_7$ ceramics does not permit energy to convert sufficiently to be used for densification. The average grain size also remains small, which only increases from 61 nm to 96 nm as the temperature increases from 1100 °C to 1300 °C. This can be explained by the rapid heating that suppresses the surface diffusion and thereby minimizes grain growth [26]. Thus, we concluded that microwave sintering at a high sintering temperature can produce high-density and small-grained $Gd_2Zr_2O_7$ ceramics.

To achieve controllable nano-sized grains and higher densification, we systematically studied the relationship between the sintering time and the grain boundary diffusion. Under a constant sintering time (60 min), the relative density and the grain growth of $Gd_2Zr_2O_7$ ceramics as a function of sintering temperature are shown in Fig. 3. As the sintering temperature increases from 1100 °C to 1300 °C, the relative density increases from 88% to 95%, which is aligned with the trend of the grain growth. This can be explained by the close connection between the elimination of open pores due to sintering and the coarsening of grains [16]. Notably, a significant increase in the grain size was observed above 1250 °C. As a consequence, at 1300 °C, the fabricated sample has large grains (> 120 nm) and high density (95%). On the other hand, Fig. 3 also suggests that nano-grained ceramics (62 nm-92 nm) with high density (> 90%) can be reasonably obtained from 1150°C to 1250 °C.

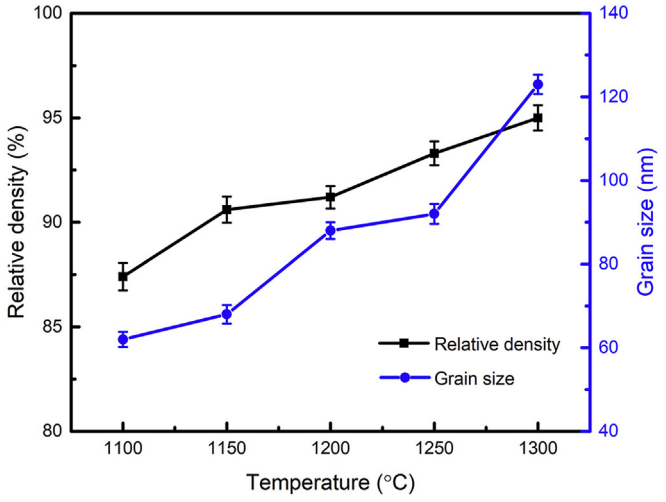

Fig. 3. Grain growth and relative density of the $Gd_2Zr_2O_7$ ceramics fabricated at different temperature for 60 min. Data were plotted as a function of sintering temperature.

The microstructures of $Gd_2Zr_2O_7$ ceramics sintering for 60 min are shown in Fig. 4. Firstly, at a high temperature (1300 °C), the sintered samples have populated circular- and prismatic-shape grains with almost no porosities (relative density of 95%) (Fig. 4(e)). Compared to sintering for 30 min, there is an obvious growth in the average grain size from 96 nm to 123 nm (Table 1, Figs. 2(e) and 4(e)), which may be due to the enhancement by the electric field in the intermediate stages that accelerates densification [38]. Similar phenomena were also observed in other systems [39,40]. In contrary, at lower temperatures (1100–1200 °C), there is a weaker correlation between microstructure and sintering time. For instance, increasing sintering time from 30 to 60 min under 1100 °C (Table 1) only resulted in a minimal grain growth of 1 nm. Thus, we concluded that a longer sintering time under low temperatures (< 1250 °C) can help normal densification with no noticeable grain growth; while at higher temperatures (> 1250 °C), there is a stronger correlation between grain growth and sintering time. Therefore, both time and temperature can effectively impact densification and grain growth during the microwave sintering process.

In order to separate the contribution of time from temperature, a more comprehensive investigation was conducted and the results were summarized in Table 1. The grain size, and the relative density as functions of sintering temperature and time were shown in Fig. 5, and Fig. 6, respectively. Both the grain growth and the densification have positive correlations with sintering time. A short sintering time (10 min) between 1250 °C and 1300 °C can produce samples with average grain size from 85 nm to 93 nm, as shown in Fig. 5. The microstructures of these ceramics (Fig. 7) have both little pores and homogenous nano-grains. Sintering for a long time (90 min) at 1100 °C, 1150 °C, and 1200 °C led to ceramics with average grain size of 66 nm, 85 nm, and 95 nm, respectively (Fig. 5), and density all above 90% (Fig. 6). This suggests that a long sintering time exceeding 60 min can contribute remarkably to densification at low temperatures. Furthermore, it can be seen that grains grow enormously from sintering for 60–90 min at 1150 °C, while densification only improves slowly (also for temperature > 1150 °C). This may be due to that the forward diffusion of ions is promoted and the grain growth is accelerated [41]. Lastly, the sample sintered at 1250 °C for 10 min has a higher density than that of the sample sintered at 1200 °C for 30 min (Fig. 6). This suggests that the diffusion mechanisms are more sensitive to the electric properties which affect density [41]. Therefore, we concluded that either an extended sintering time (30–90 min) below 1250 °C or a short holding time (10–60 min) at high temperature can fabricate samples

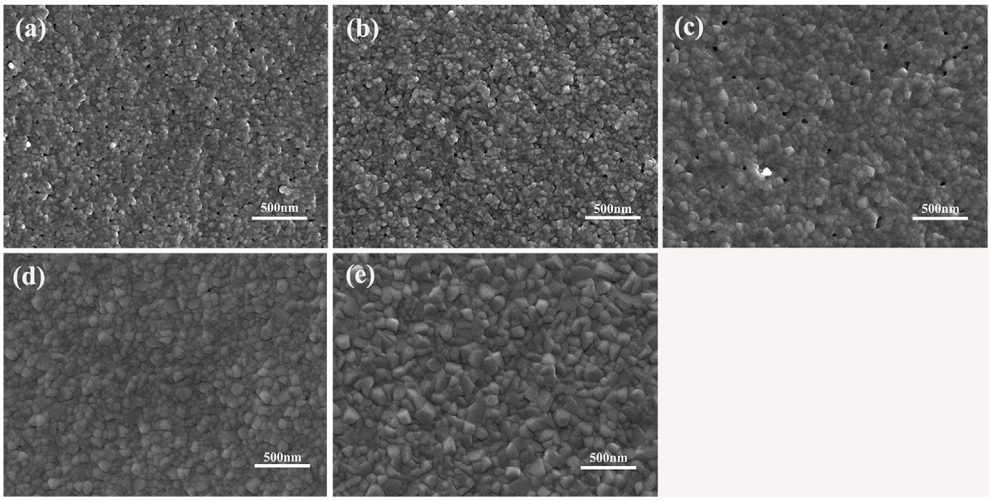

Fig. 4. Scanning electron microscopy (SEM) images of $Gd_2Zr_2O_7$ ceramics sintered for 60 min at (a) 1100 °C, (b) 1150 °C, (c) 1200 °C, (d) 1250 °C, and (e) 1300 °C.

Table 1
Sintering conditions, relative density and average grain size of $Gd_2Zr_2O_7$ ceramics.

Sample	Microwave sintering temperature (°C)	Holding time (minutes)	Relative density (%)	Average grain size (nm)
1	1100	30	86	61
2	1100	60	88	62
3	1100	90	91	66
4	1150	30	89	65
5	1150	60	91	68
6	1150	90	92	87
7	1200	30	91	84
8	1200	60	91	88
9	1200	90	92	92
10	1250	10	91	87
11	1250	30	92	88
12	1250	60	93	92
13	1300	10	92	93
14	1300	30	93	96
15	1300	60	95	123

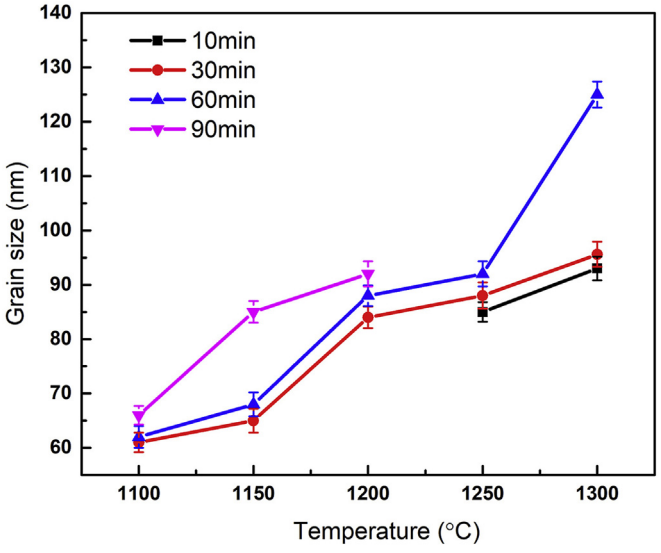

Fig. 5. Grain size of $Gd_2Zr_2O_7$ ceramics prepared with different holding time as a function of sintering temperature.

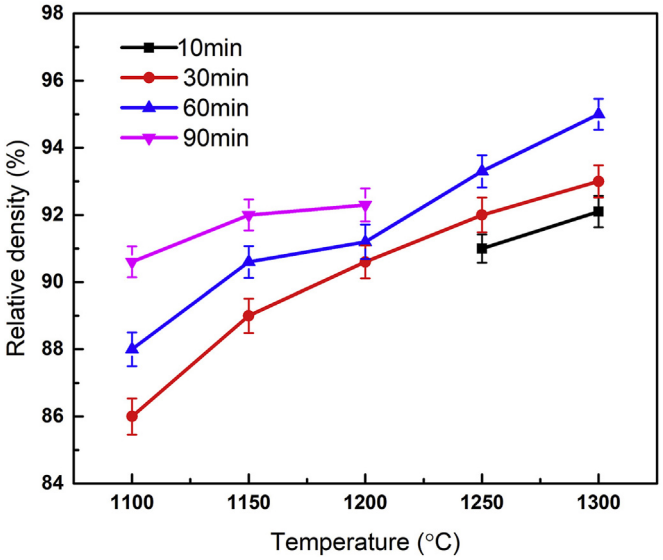

Fig. 6. Relative density of $Gd_2Zr_2O_7$ ceramics prepared in different holding time as a function of sintering temperature.

with small nano-grains (< 100 nm).

The increased densification and the uniform nano-grain distribution resulted from microwave sintering can be understood by the coupled effect of ions and electric dipoles, which is closely related to the dielectric properties and defect structures of the target materials [26]. Due to the volumetric heating and reduced activation for the forward jump of ions (a high barrier for a reversed jump), microwave sintering can be applied at much lower temperature for shorter sintering time that reduces energy consumption compared to conventional sintering [16]. The much lower activation energy for grain growth in the cubic phase makes the densification be enhanced without having the grain size significantly grow [42]. During microwave sintering, thermal energy is generated from the direct interaction between the particles and the electromagnetic field due to the dielectric loss of ceramic materials to achieve sintering and densification. The dielectric loss with frequency dependence is shown as follows,

$$\tan\delta = \frac{\varepsilon_r''}{\varepsilon_r'} = \frac{(\varepsilon_{r0} - \varepsilon_{r\infty})(\omega\tau_0)}{\varepsilon_{r0} + \varepsilon_{r\infty}\omega^2\tau_0} \quad (1)$$

The dielectric constant ε_r, shows a curving frequency dependence on a logarithm scale and in the low-frequency range reaches large values

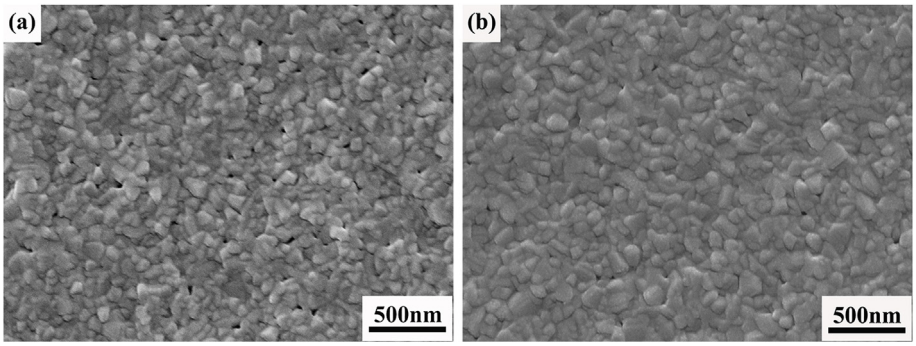

Fig. 7. Scanning electron microscopy (SEM) images of $Gd_2Zr_2O_7$ ceramics sintered at (a) 1250 °C and (b) 1300 °C for 10 min.

due to the electrolyte-electrode interfacial polarization process [43,44]. The value of tanδ is composed of a single peak, which shifts to the high-frequency region with a stronger intensity as temperature increases [44]. This can explain why we obtained dense ceramics at high temperature after short sintering time. When at a relatively low temperature, long sintering time may compensate the loss of dielectric performance to assist densification.

Thus, extending sintering time (60–90 min) at low temperature is a promising approach to accelerate the diffusion of ions between sample particles. As a result, dense ceramics (> 90%) with fine microstructures (66 nm-92 nm) were fabricated at low temperatures from 1100 °C to 1200 °C after extending the holding time. As sintering temperature increases, the forward jump of diffusion activation energy is effectively promoted that produces larger grains. Thus, a long holding time of 60 or 90 min at high temperatures (> 1250 °C) has an adverse effect on controlling the grain size in nanometer. Thus, a short sintering time (10 min) is required when heating above 1250 °C to help control the grain size (87 nm-93 nm) and yield high relative density (> 90%). In addition, dense ceramics (> 90%) with grain sizes from 84 nm to 93 nm could be obtained after sintering for 30 min at between 1200 °C and 1300 °C. Both the sintering time and temperature can change the dielectric properties of ceramics, which may affect the diffusion behavior of $Gd_2Zr_2O_7$ under microwave sintering. The dielectric properties of the ceramics are strongly associated with porosity and grain size [24], which in turn influence the microstructure. The detailed mechanism of microwave sintering of the $Gd_2Zr_2O_7$ nanoceramics will be investigated in our future work.

4. Conclusion

High-density (> 90%) and nano grain-sized (< 100 nm) $Gd_2Zr_2O_7$ ceramics were obtained at 1100°C-1300 °C after short holding time (10–90 min) by using the pressureless sintering method under the electromagnetic field. Samples sintered by microwave sintering exhibit higher density (> 90%) and smaller average grain-size (66 nm-96 nm) compared to those of samples made by conventional sintering. Extending sintering time at low temperatures (< 1250 °C) and limiting sintering time at high temperatures (> 1250 °C) both improve densification with minimal grain growth. Particularly, $Gd_2Zr_2O_7$ ceramics with relative density above 91% and average grain size of 66 nm can be prepared by sintering at 1100 °C for 90 min. Thus, we concluded that microwave sintering method can provide an efficient and economic pathway in immobilizing radionuclides in the ceramic matrices with short processing time.

Acknowledgements

This work was supported by the National Natural Science Foundation of the People's Republic of China under Grant Nos. 11505122 and 11775152, the Science and Technology Innovation Team of Sichuan province under Grant NO.15CXTD0025, and the Key Applied Basic Research (2017JY0329) of Sichuan province. X. Guo acknowledges the institutional fund from the Department of Chemistry at Washington State University.

Appendix A. Supplementary data

Supplementary data to this article can be found online at https://doi.org/10.1016/j.ceramint.2019.02.173.

References

[1] A. Ringwood, S. Kesson, N. Ware, W. Hibberson, A. Major, Immobilisation of high level nuclear reactor wastes in SYNROC, Nature 278 (1979) 219.
[2] G.R. Lumpkin, Ceramic waste forms for actinides, Elements 2 (2006) 365–372.
[3] W.J. Weber, A. Navrotsky, S. Stefanovsky, E.R. Vance, E. Vernaz, Materials science of high-level nuclear waste immobilization, MRS Bull. 34 (2009) 46–53.
[4] X. Guo, R.K. Kukkadapu, A. Lanzirotti, M. Newville, M.H. Engelhard, S.R. Sutton, A. Navrotsky, Charge-coupled substituted garnets $(Y_{3-x}Ca_{0.5x}M_{0.5x})Fe_5O_{12}$ (M = Ce, Th): structure and stability as crystalline nuclear waste forms, Inorg. Chem. 54 (2015) 4156–4166.
[5] X. Guo, A. Navrotsky, R.K. Kukkadapu, M.H. Engelhard, A. Lanzirotti, M. Newville, E.S. Ilton, S. Sutton, H. Xu, Structure and thermodynamics of uranium containing iron garnets, Geochem. Cosmochim. Acta 189 (2016) 269–281.
[6] X.-M. Bai, A.F. Voter, R.G. Hoagland, M. Nastasi, B.P. Uberuaga, Efficient annealing of radiation damage near grain boundaries via interstitial emission, Science 327 (2010) 1631–1634.
[7] Y.-Q. Chang, Q. Guo, J. Zhang, L. Chen, Y. Long, F.-R. Wan, Irradiation effects on nanocrystalline materials, Front. Mater. Sci. 7 (2013) 143–155.
[8] J. Wen, C. Sun, P.P. Dholabhai, Y. Xia, M. Tang, D. Chen, D.Y. Yang, Y.H. Li, B.P. Uberuaga, Y.Q. Wang, Temperature dependence of the radiation tolerance of nanocrystalline pyrochlores $A_2Ti_2O_7$ (A = Gd, Ho and Lu), Acta Mater. 110 (2016) 175–184.
[9] T.D. Shen, S. Feng, M. Tang, J.A. Valdez, Y. Wang, K.E. Sickafus, Enhanced radiation tolerance in nanocrystalline $MgGa_2O_4$, Appl. Phys. Lett. 90 (2007) 263115.
[10] S. Dey, J.W. Drazin, Y. Wang, J.A. Valdez, T.G. Holesinger, B.P. Uberuaga, R.H. Castro, Radiation tolerance of nanocrystalline ceramics: insights from yttria stabilized zirconia, Sci. Rep. 5 (2015) 7746.
[11] J. Zhang, J. Lian, A.F. Fuentes, F. Zhang, M. Lang, F. Lu, R.C. Ewing, Enhanced radiation resistance of nanocrystalline pyrochlore $Gd_2(Ti_{0.65}Zr_{0.35})_2O_7$, Appl. Phys. Lett. 94 (2009) 243110.
[12] K. Sickafus, L. Minervini, R. Grimes, J. Valdez, M. Ishimaru, F. Li, K. McClellan, T. Hartmann, Radiation tolerance of complex oxides, Science 289 (2000) 748–751.
[13] W.J. Weber, R.C. Ewing, Plutonium immobilization and radiation effects, Science 289 (2000) 2051–2052.
[14] P. Morgan, D. Clarke, C. Jantzen, A. Barker, High-alumina tailored nuclear waste ceramics, J. Am. Ceram. Soc. 64 (1981) 249–258.
[15] Z. Huang, Z. Cao, K. Shi, J. Qi, M. Zhou, Z. Tang, W. Han, X. Diao, J. Tang, T. Lu, Synthesis and densification of $Gd_2Zr_2O_7$ nanograin ceramics prepared by field assisted sintering technique, J. Nucl. Mater. 495 (2017) 164–171.
[16] K. Lu, Sintering of nanoceramics, Int. Mater. Rev. 53 (2008) 21–38.
[17] D. Ehre, E.Y. Gutmanas, R. Chaim, Densification of nanocrystalline MgO ceramics by hot-pressing, J. Eur. Ceram. Soc. 25 (2005) 3579–3585.
[18] T. Wangle, V. Tyrpekl, M. Cologna, J. Somers, Simulated UO_2 fuel containing CsI by spark plasma sintering, J. Nucl. Mater. 466 (2015) 150–153.
[19] M. Zhou, Z. Huang, J. Qi, N. Wei, D. Wu, Q. Zhang, S. Wang, Z. Feng, T. Lu, Densification and grain growth of $Gd_2Zr_2O_7$ nanoceramics during pressureless sintering, J. Eur. Ceram. Soc. 37 (2017) 1059–1065.
[20] T.T. Meek, R.D. Blake, J.J. Petrovic, Microwave sintering of Al_2O_3 and Al_2O_3-SiC whisker composites, 11th Annual Conference on Composites and Advanced Ceramic Materials: Ceramic Engineering and Science Proceedings, Wiley Online Library, 1987, pp. 861–871.
[21] K.H. Brosnan, G.L. Messing, D.K. Agrawal, Microwave sintering of alumina at 2.45 GHz, J. Am. Ceram. Soc. 86 (2003) 1307–1312.

[22] D. Upadhyaya, A. Ghosh, G. Dey, R. Prasad, A. Suri, Microwave sintering of zirconia ceramics, J. Mater. Sci. 36 (2001) 4707–4710.
[23] J. Cheng, D. Agrawal, Y. Zhang, R. Roy, Microwave reactive sintering to fully transparent aluminum oxynitride (AlON) ceramics, J. Mater. Sci. Lett. 20 (2001) 77–79.
[24] A. Birnboim, D. Gershon, J. Calame, A. Birman, Y. Carmel, J. Rodgers, B. Levush, Y.V. Bykov, A. Eremeev, V. Holoptsev, Comparative study of microwave sintering of zinc oxide at 2.45, 30, and 83 GHz, J. Am. Ceram. Soc. 81 (1998) 1493–1501.
[25] K.E. Haque, Microwave energy for mineral treatment processes – a brief review, Int. J. Miner. Process. 57 (1999) 1–24.
[26] M. Oghbaei, O. Mirzaee, Microwave versus conventional sintering: a review of fundamentals, advantages and applications, J. Alloy. Comp. 494 (2010) 175–189.
[27] S.J. Penn, N.M. Alford, A. Templeton, X. Wang, M. Xu, M. Reece, K. Schrapel, Effect of porosity and grain size on the microwave dielectric properties of sintered alumina, J. Am. Ceram. Soc. 80 (1997) 1885–1888.
[28] P. Yadoji, R. Peelamedu, D. Agrawal, R. Roy, Microwave sintering of Ni–Zn ferrites: comparison with conventional sintering, Mater. Sci. Eng. B 98 (2003) 269–278.
[29] D. Agrawal, Microwave sintering of ceramics, composites, metals, and transparent materials, J. Mater. Educ. 19 (1997) 49–58.
[30] D.E. Clark, D.C. Folz, J.K. West, Processing materials with microwave energy, Mater. Sci. Eng., A 287 (2000) 153–158.
[31] C. Leonelli, P. Veronesi, L. Denti, A. Gatto, L. Iuliano, Microwave assisted sintering of green metal parts, J. Mater. Process. Technol. 205 (2008) 489–496.
[32] R. R Menezes, P.M. Souto, R.H. Kiminami, Microwave hybrid fast sintering of porcelain bodies, J. Mater. Process. Technol. 190 (2007) 223–229.
[33] C.L. Huang, J.J. Wang, C.Y. Huang, Sintering behavior and microwave dielectric properties of nano alpha-alumina, Mater. Lett. 59 (2005) 3746–3749.
[34] X. Lu, Y. Ding, H. Dan, S. Yuan, X. Mao, L. Fan, Y. Wu, Rapid synthesis of single phase $Gd_2Zr_2O_7$ pyrochlore waste forms by microwave sintering, Ceram. Int. 40 (2014) 13191–13194.
[35] Z. Huang, J. Qi, M. Zhou, Y. Gong, Q. Shi, M. Yang, W. Han, Z. Cao, S. Peng, T. Lu, A facile solvothermal method for high-quality $Gd_2Zr_2O_7$ nanopowder preparation, Ceram. Int. 44 (2018) 1334–1342.
[36] Z. Huang, J. Qi, L. Zhou, Z. Feng, X. Yu, Y. Gong, M. Yang, Q. Shi, N. Wei, T. Lu, Fast crystallization of amorphous $Gd_2Zr_2O_7$ induced by thermally activated electron-beam irradiation, J. Appl. Phys. 118 (2015) 214901.
[37] L. Zhou, Z. Huang, J. Qi, Z. Feng, D. Wu, W. Zhang, X. Yu, Y. Guan, X. Chen, L. Xie, K. Sun, Thermal-driven fluorite-pyrochlore-fluorite phase transitions of $Gd_2Zr_2O_7$ ceramics probed in large range of sintering temperature, Metall. Mater. Trans. 47 (2016) 623–630.
[38] J. Croquesel, D. Bouvard, J.M. Chaix, C.P. Carry, S. Saunier, S. Marinel, Direct microwave sintering of pure alumina in a single mode cavity: grain size and phase transformation effects, Acta Mater. 116 (2016) 53–62.
[39] S. Vijayan, H. Varma, Microwave sintering of nanosized hydroxyapatite powder compacts, Mater. Lett. 56 (2002) 827–831.
[40] Y.V. Bykov, S.V. Egorov, A.G. Eremeev, K.I. Rybakov, V.E. Semenov, A.A. Sorokin, S.A. Gusev, Evidence for microwave enhanced mass transport in the annealing of nanoporous alumina membranes, J. Mater. Sci. 36 (2001) 131–136.
[41] M. Yan, J. Hu, Microwave sintering of high-permeability $(Ni_{0.20}Zn_{0.60}Cu_{0.20})Fe_{1.98}O_4$ ferrite at low sintering temperatures, J. Magn. Magn Mater. 305 (2006) 171–176.
[42] S.A. Nightingale, H.K. Worner, D.P. Dunne, Microstructural development during the microwave sintering of yttria-zirconia ceramics, J. Am. Ceram. Soc. 80 (1997) 394–400.
[43] P. Sarkar, P.S. Nicholson, Electric field relaxation studies in the CeO_2-Y_2O_3 system, J. Phys. Chem. Solid. 50 (1989) 197–206.
[44] H. Yamamura, H. Nishino, K. Kakinuma, Relationship between oxide-ion conduction and dielectric properties of $Gd_2Zr_2O_7$ having a fluorite-type structure, Jpn. J. Appl. Phys. 47 (2008) 5521.